doi:10.1246/cl.2012.116
Published on the web December 30, 2011

A *mer*-Triaqua Rh Complex with a Terpyridine Ligand

Daisuke Inoki,[1,2] Takahiro Matsumoto,[1,3] Hidetaka Nakai,[1,3] and Seiji Ogo*[1,2,3]
[1]*Department of Chemistry and Biochemistry, Graduate School of Engineering, Kyushu University, 744 Moto-oka, Nishi-ku, Fukuoka 819-0395*
[2]*Core Research for Evolutional Science and Technology (CREST), Japan Science and Technology Agency (JST), Kawaguchi Center Building, 4-1-8 Honcho, Kawaguchi, Saitama 332-0012*
[3]*International Institute for Carbon-Neutral Energy Research (I^{2}CNER), Kyushu University, 744 Moto-oka, Nishi-ku, Fukuoka 819-0395*

(Received November 14, 2011; CL-111104; E-mail: ogotcm@mail.cstm.kyushu-u.ac.jp)

We report the synthesis of a *mer*-triaqua Rh^{III} complex using terpyridine as a meridional tridentate ligand. This is the first example of a structurally characterized six-coordinated *mer*-triaqua complex for any second- or third-row element from the main transition-metal groups (groups 5–11). This is also the first example of a structurally characterized *mer*-triaqua complex with terpyridine for any transition metal. Acid dissociation constants, pK_{a1} and pK_{a2}, of the triaqua complex are determined to be 3.0 and 6.9, respectively.

Transition-metal aqua complexes are attractive as good synthetic precursors since the aqua ligands are easily replaceable with other ligands.[1–6] Although many first-row *fac*- and *mer*-triaqua transition-metal complexes have been reported,[2,3] no X-ray structure of *mer*-triaqua complexes for any of the second- or third-row elements of the main section of the transition metals (groups 5–11) has been reported until now (Figure 1). These elements, of course, incorporate the catalytically important precious metals and so a precious metal *mer*-triaqua complex would be useful for constructing novel catalytic topologies. Here, we report the synthesis of just such a *mer*-triaqua Rh^{III} complex, using the *mer*-type terpyridine ligand. This complex is also notable as being the first example of a structurally characterized terpyridine-bearing *mer*-triaqua compound.

A triaqua complex [Rh^{III}(terpy)(H$_2$O)$_3$](NO$_3$)$_3$ {[**1**](NO$_3$)$_3$, terpy: 2,2′:6′,2″-terpyridine} was synthesized by the treatment of [Rh^{III}(terpy)Cl$_3$] with three equivalents of AgNO$_3$ in H$_2$O at pH 2.0. Complex **1** is based on a Rh^{III} core tethered to a terpyridine ligand, and has three aqua ligands. Recrystallization of [**1**](NO$_3$)$_3$ in CH$_3$OH gave pale yellow crystals suitable for X-ray analysis (Figure 2).[7]

The X-ray structure reveals that the Rh atom adopts a distorted-octahedral coordination including the three aqua ligands in a *mer*-configuration. The bond lengths between the Rh atom and the O atoms of the aqua ligands are 2.013(2), 2.049(2), and 2.022(2) Å for Rh1–O1, Rh1–O2, and Rh1–O3, respectively. These bond lengths are slightly shorter than those found in a monohydroxido diaqua Rh^{III} complex [Rh^{III}(terpy)(OH)(H$_2$O)$_2$](NO$_3$)$_2$ {[**2**](NO$_3$)$_2$} {2.060(1) and 2.057(1) Å, Figure S1 in Supporting Information}[8,9] and much shorter than those found in a *fac*-triaqua Rh^{III} complex [Rh^{III}(C$_5$Me$_5$)(H$_2$O)$_3$]$^{2+}$ {2.213(8), 2.137(8), and 2.131(8) Å}.[5b] The shorter Rh–O bond lengths in **1** seem to originate from the lower electron density of the Rh^{III} center: the negative C$_5$Me$_5$ ligand has stronger electron-donating ability than the neutral terpy ligand.

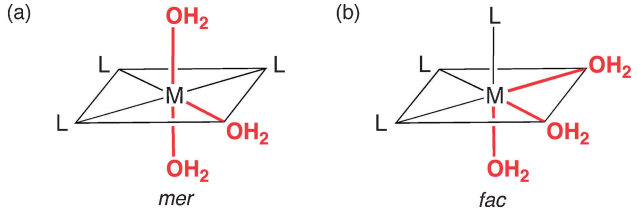

Figure 1. (a) *mer*- and (b) *fac*-Triaqua complexes. M: transition metals. L: supporting ligands.

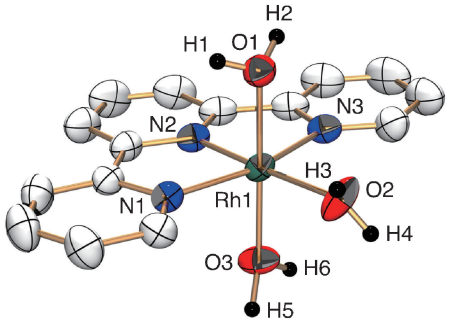

Figure 2. An ORTEP drawing of [**1**](NO$_3$)$_3$·1.5H$_2$O with ellipsoids at 50% probability. The counter anions (NO$_3$), solvents (H$_2$O), and hydrogen atoms of terpy are omitted for clarity. Selected interatomic distances (l/Å) and angles (ϕ/°): Rh1–O1 = 2.013(2), Rh1–O2 = 2.049(2), Rh1–O3 = 2.022(2), Rh1–N1 = 2.033(2), Rh1–N2 = 1.922(2), Rh1–N3 = 2.037(2), O1–Rh1–O2 = 86.15(7), O2–Rh1–O3 = 93.01(8), O1–Rh1–O3 = 178.09(7), O1–Rh1–N1 = 89.69(7), O1–Rh1–N2 = 92.79(7), O1–Rh1–N3 = 89.94(7), O2–Rh1–N1 = 100.26(7), O2–Rh1–N2 = 177.90(8), O2–Rh1–N3 = 96.63(8), O3–Rh1–N1 = 88.78(7), O3–Rh1–N2 = 88.12(8), O3–Rh1–N3 = 91.86(8), N1–Rh1–N2 = 81.54(8), N1–Rh1–N3 = 163.05(8), N2–Rh1–N3 = 81.55(9).

The successive deprotonation processes of **1**, which are associated with pK_{a1} and pK_{a2}, were clearly monitored by ^{1}H NMR (Figure 3) and UV–vis spectroscopy (Figures 4 and 5) by changing the pH (pD) of the solution. The pK_{a1} and pK_{a2} values of **1** were determined to be 3.0 and 6.9, respectively, in the range of pH (pD) about 1–9. ^{1}H NMR spectrum of the terpy ligand in **1** in D$_2$O at pD 1.2 shows the signals at 8.12 (5- and 5″-*H*), 8.56 (4- and 4″-*H*), 8.61–8.75 (3-, 3′-, 4′-, 5′-, and 3″-*H*), and 9.17 (6- and 6″-*H*) ppm, which are assigned by H–H COSY (Figure S2 in Supporting Information).[9] As shown in Figure 3, these signals are shifted upfield to 7.97, 8.40, 8.45–8.59, and

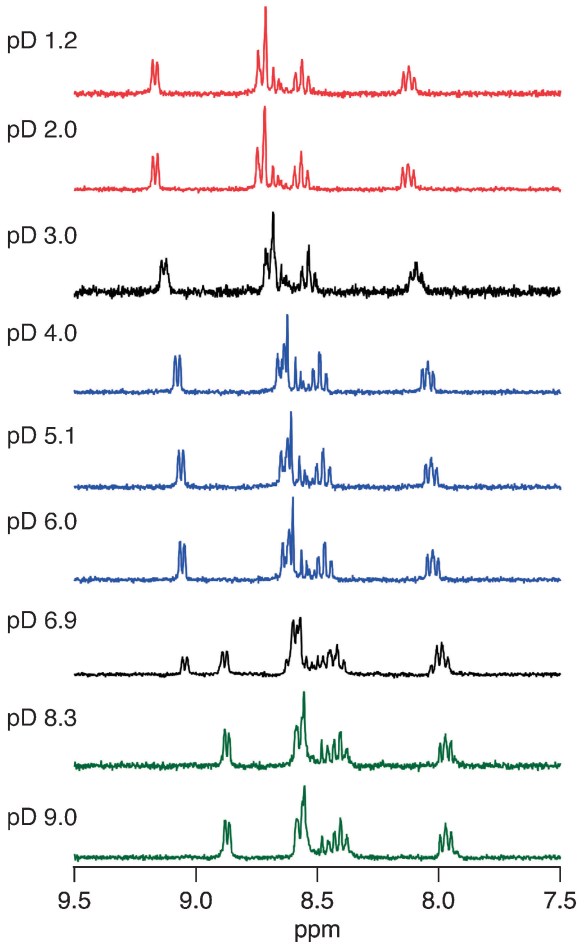

Figure 3. pD-dependent ^{1}H NMR spectra of **1** (1.0 mM) in D_2O in the range of pD 1.2–9.0. Experiments were performed by the titration of **1** with NaOD/D_2O.

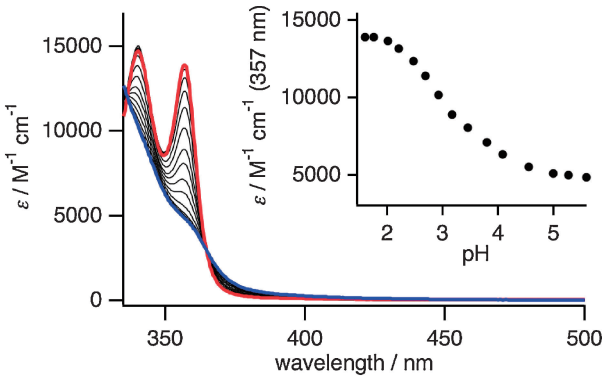

Figure 4. pH-dependent UV–vis spectra of **1** (54 μM) in H_2O in the range of pH 1.6–5.6. The inset gives a plot of absorbance ($\lambda = 357$ nm) versus pH. Experiments were performed by the titration of **1** with NaOH/H_2O.

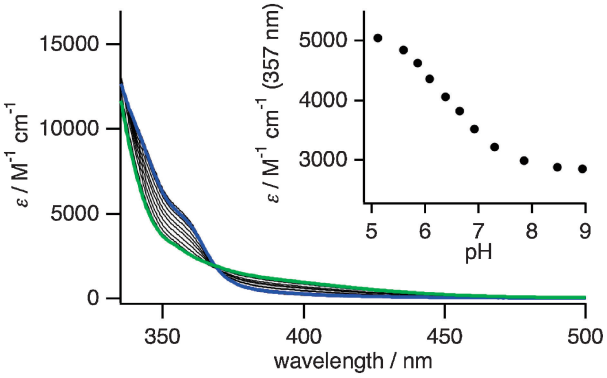

Figure 5. pH-dependent UV–vis spectra of **1** (54 μM) in H_2O in the range of pH 5.0–9.0. The inset gives a plot of absorbance ($\lambda = 357$ nm) versus pH. Experiments were performed by the titration of **1** with NaOH/H_2O.

8.87 ppm by increasing the pD value from 1.2 to 9.0. The distinct spectral changes are observed around pD 3.0 and 6.9, and the changes are reversible.

The pK_a values of **1** determined by ^{1}H NMR titration experiments are consistent with those determined by UV–vis spectroscopic titration. The pH-dependent UV–vis spectra of **1** show that the sharp intense bands at 340 and 357 nm disappear by increasing the pH value from 1.6 to 5.6 (Figure 4). When the pH is further increased to 9.0, a shoulder band around 360 nm decreases with an isosbestic point at 369 nm (Figure 5). These UV–vis spectral changes are also reversible as was confirmed in the ^{1}H NMR titration experiments.

Based on the isolation and structural characterization of the monohydroxido diaqua Rh^{III} complex [**2**]$(NO_3)_2$, it is proposed that the first deprotonation process of **1**, which is associated with pK_{a1}, generates **2** (eq 1). In the range of the second- or third-row triaqua transition-metal complexes of groups 8 and 9, the pK_{a1} values previously reported for the triaqua transition-metal complexes, which include multi-deprotonation in one step, are as follows: *fac*-triaqua organometallic complexes $[Ru^{II}(C_6H_6)(H_2O)_3]^{2+}$ (3.5),[4a] $[Ru^{II}(C_6Me_6)(H_2O)_3]^{2+}$ (3.5),[1] $[Rh^{III}(C_5Me_5)(H_2O)_3]^{2+}$ (3.6),[5a] and $[Ir^{III}(C_5Me_5)(H_2O)_3]^{2+}$ (2.8);[5f] *fac*-triaqua 1,4,7-triazacyclononane (tacn) complexes $[Rh^{III}(tacn)(H_2O)_3]^{3+}$ (6.1)[5c] and $[Ir^{III}(tacn)(H_2O)_3]^{3+}$ (5.9);[5c] *mer*-triaqua terpy complexes $[Ru^{III}(terpy)(H_2O)_3]^{3+}$ (2.1),[6b] $[Os^{III}(terpy)(H_2O)_3]^{3+}$ (2.2),[6a] $[Ru^{II}(terpy)(H_2O)_3]^{2+}$ (5.3),[6b] and $[Os^{II}(terpy)(H_2O)_3]^{2+}$ (6.3).[6a] Thus, the pK_{a1} value (3.0) of the *mer*-triaqua Rh^{III} terpy complex **1** is higher than those reported for the *mer*-triaqua Ru^{III} and Os^{III} terpy complexes and lower than those reported for *mer*-triaqua Ru^{II} and Os^{II} terpy complexes.

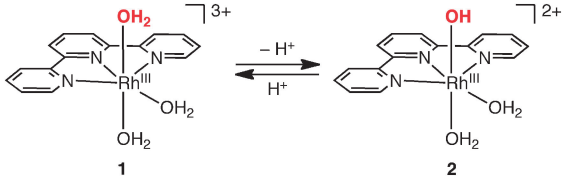

1 2 (1)

With regard to the second deprotonation species {dominant species at pH values higher than 6.9 (pK_{a2})}, the possible species to be formed in our system is a mononuclear dihydroxido complex, dinuclear bis(μ-hydroxido) complex, or the other deprotonated species. However, at the moment, the isolation and characterization of the two deprotonated species has not been achieved yet.

In conclusion, we have first characterized the *mer*-triaqua Rh^{III} terpy complex **1** by X-ray analysis. This is also the first example of a structurally characterized *mer*-triaqua complex

with terpyridine for any transition metal. The *mer*-triaqua arrangement and unique pK_a values of **1** would be useful to construct a novel pH-dependent catalyst in aqueous media.

This work was supported by the World Premier International Research Center Initiative (WPI Program), Grants-in-Aid: Nos. 18065017 (Chemistry of *Concerto* Catalysis), 19205009, and 23655053, the Global COE Program, "Science for Future Molecular Systems" from the Ministry of Education, Culture, Sports, Science and Technology (MEXT), Japan and the Basic Research Programs CREST Type, "Development of the Foundation for Nano-Interface Technology" from JST, Japan.

References and Notes

1 U. Kölle, *Coord. Chem. Rev.* **1994**, *135–136*, 623.
2 a) L. O. Spreer, I. Shah, *Inorg. Chem.* **1981**, *20*, 4025. b) G. C. Silver, W. C. Trogler, *J. Am. Chem. Soc.* **1995**, *117*, 3983. c) M. Montag, C. R. Clough, P. Müller, C. C. Cummins, *Chem. Commun.* **2011**, *47*, 662.
3 a) P. Lainé, A. Gourdon, J.-P. Launay, *Inorg. Chem.* **1995**, *34*, 5129. b) P. Kapoor, A. Pathak, P. Kaur, P. Venugopalan, R. Kapoor, *Transition Met. Chem.* **2004**, *29*, 251. c) V. M. Leovac, L. S. Jovanović, V. Divjaković, A. Pevec, I. Leban, T. Armbruster, *Polyhedron* **2007**, *26*, 49. d) S. K. Padhi, R. Sahu, V. Manivannan, *Polyhedron* **2008**, *27*, 2221.
4 a) M. Stebler-Röthlisberger, W. Hummel, P.-A. Pittet, H.-B. Bürgi, A. Ludi, A. E. Merbach, *Inorg. Chem.* **1988**, *27*, 1358. b) S. Ogo, T. Abura, Y. Watanabe, *Organometallics* **2002**, *21*, 2964.
5 a) U. Kölle, W. Kläui, *Z. Naturforsch., B* **1991**, *46*, 75. b) M. S. Eisen, A. Haskel, H. Chen, M. M. Olmstead, D. P. Smith, M. F. Maestre, R. H. Fish, *Organometallics* **1995**, *14*, 2806. c) F. Galsbøl, C. H. Petersen, K. Simonsen, *Acta Chem. Scand.* **1996**, *50*, 567. d) S. Ogo, O. Buriez, J. B. Kerr, R. H. Fish, *J. Organomet. Chem.* **1999**, *589*, 66. e) S. Ogo, N. Makihara, Y. Watanabe, *Organometallics* **1999**, *18*, 5470. f) N. Makihara, S. Ogo, Y. Watanabe, *Organometallics* **2001**, *20*, 497.
6 a) D. W. Pipes, T. J. Meyer, *Inorg. Chem.* **1986**, *25*, 4042. b) S. A. Adeyemi, A. Dovletoglou, A. R. Guadalupe, T. J. Meyer, *Inorg. Chem.* **1992**, *31*, 1375.
7 Crystal data for $[\mathbf{1}](NO_3)_3 \cdot 1.5H_2O$: $C_{15}H_{20}N_6O_{13.5}Rh$, fw 603.26, monoclinic, $a = 17.604(4)$ Å, $b = 10.955(2)$ Å, $c = 24.274(5)$ Å, $\alpha = 90°$, $\beta = 102.155(2)°$, $\gamma = 90°$, $V = 4576(1)$ Å^3, $T = 293.2$ K, space group $C2/c$, $Z = 8$, 25141 reflections measured, 5229 independent reflections ($R_{int} = 0.025$), $R_1 = 0.030$, $wR = 0.072$. The goodness of fit on F^2 was 1.000. CCDC number CCDC 841913.
8 D. Inoki, T. Matsumoto, H. Hayashi, K. Takashita, H. Nakai, S. Ogo, *Dalton Trans.* **2012**, Advance Article. doi:10.1039/c1dt11599e.
9 Supporting Information is available electronically on the CSJ-Journal Web site, http://www.csj.jp/journals/chem-lett/index.html.

